동축공기 수소확산 화염에서의 화염과 와류의 상호작용 실험연구

김문기* · 오정석* · 최영일* · 윤영빈**†

Experimental Study on Flame-Vortex Interactions in Turbulent Hydrogen Non-premixed Flames with Coaxial Air

Munki Kim, Jeong-suk Oh, Young-il Choi and Youngbin Yoon

ABSTRACT

This paper investigates the effects of acoustic forcing on NOx emissions and mixing process in the near field region of turbulent hydrogen nonpremixed flames. The resonance frequency was selected to force the coaxial air jet acoustically, because the resonance frequency is effective to amplify the forcing amplitude and reduce NOx emissions. When the resonance frequency is acoustically excited, a streamwise vortex is formed in the mixing layer between the coaxial air jet and coflowing air. As the vortex develops downstream, it entrains both ambient air and combustion products into the coaxial air jet to mix well. In addition, the strong vortex pulls the flame surface toward the coaxial air jet, causing intense chemical reaction. Acoustic excitation also causes velocity fluctuations of coaxial air jet as well as fuel jet but, the maximum value of centerline fuel velocity fluctuation occurs at the different phases of ϕ=180° for nonreacting case and ϕ=0° for reacting case. Since acoustic excitation enhances the mixing rate of fuel and air, the line of the stoichiometric mixture fraction becomes narrow. Finally, acoustic forcing at the resonance frequency reduces the normalized flame length by 15 % and EINOx by 25 %, compared to the flame without acoustic excitation.

Key Words : Acoustic forcing, NOx emission, Coaxial air, Resonance frequency

기 호 설 명

u_F	Fuel velocity	τ_R	Flame residence time
u_A	Coaxial air velocity	I_{ac}	Acetone PLIF intensity
L_f	Flame length	$I_{ac\phi}$	Pure Jet Acetone PLIF intensity
d_F	Fuel nozzle inner diameter	f_{ac}	Acetone PLIF intensity ratio
EINOx	Emission Index of NOx		

1. Introduction

Coaxial air flames, which have the configuration of a central fuel jet and a concentric coaxial air jet, are frequently used in many practical combustion systems because of their simple and safe configuration. From many numerical and experimental studies of coaxial air flames [1-3], it is known that since a coaxial air jet provides high mixing rate and increases mixture homogeneity of fuel and air,

* 서울대학교 대학원
** 서울대학교 기계항공공학부
† 연락저자, ybyoon@snu.ac.kr

the characteristic time for NOx (Nitrogen Oxides) formation becomes shorter, resulting in a lower NOx emission than that of simple jet diffusion flames without coaxial air. In particular, Kim et al. [2, 3] conducted the NOx scaling of hydrogen nonpremixed jet flames with coaxial air and found that NOx emission index normalized by global flame residence time was proportional to the square root of global strain rate and a deviation from this tendency may be attributed to flame radiation and buoyancy effect.

Acoustic forcing used in the present study has been applied to jet flows and flames in many manners. Mostly, acoustic pulsing from a loud speaker was used to well organize large-scale vortical structures, which was closely related to physical phenomena such as vortex formation, mixing enhancement, vortex/flame interaction [4]. Meyer et al. [5] have investigated vortex formation and mixing in the near field of a driven axisymmetric jet using simultaneous planar laser-induced fluorescence (PLIF) of nitric oxide (NO) and acetone. Numerical computations of H_2/air jet flames [6] were carried out to assess preferential diffusion and stretching effects and it was found that when the flame is stretched by fuel-side vortices, a local increase in temperature was observed. Mueller and Schefer [7] performed phase-locked, PLIF measurements of OH radical in a laminar methane-air flame interacted with vortices of various sizes and strengths and their results showed that the vortex causes significant variations in the OH layer thickness. Local flame extinction has been investigated in turbulent methane jet diffusion flames interfered by the internal jet-fluid and external annulus-fluid vortices [8]. Recently, the dynamic behavior of the diffusion flame extinction and reignition during the flame-vortex interaction processes was investigated in a nitrogen-diluted hydrogen laminar diffusion flame [9].

Externally forced acoustic excitation was also used to surpass combustion instability and reduce pollutant emissions in many practical combustors. Chao et al. [10], for example, found that lifting and acoustic forcing at frequencies higher than the natural frequencies could reduce NOx emissions in partially premixed flames. Experimental results from a compact incinerator afterburner [11] and an acoustically resonant dump combustor [12] showed that acoustic excitation was efficient to enhance mixing and increase the DRE (destruction and removal efficiency) for a waste surrogate.

Although dynamics of flame-vortex interactions have been investigated to a great extent, both numerically and experimentally, most previous results mentioned above were limited to acoustically forcing a fuel jet, not a coaxial jet. Therefore, this present paper extensively describes the changes of dynamic behavior in the near field of coaxial air flames interacted with the coaxial-jet-fluid vortices, compared to those in the nonreacting cases. We also investigate how acoustic forcing affects mixing enhancement and further NOx emissions from the measurements of NOx and velocity field quantitatively.

2. Experiments

The experimental set-up consists of a flow supply section, a combustor and an exhaust gas duct as shown in Fig 1. The cross section of the combustor test-section is a 20-cm square chamber of an 80 cm in length. Nozzle geometry was composed of a fuel nozzle and a coaxial nozzle. Hydrogen was issued through the 3-mm-diameter fuel nozzle, d_F, located at the center of the combustor. The 15-mm-diameter coaxial nozzle, d_A, where coaxial air jet was injected parallel to the fuel jet was concentric to the fuel nozzle. Coflowing air was provided not only to keep the equivalence ratio constant (Φ_t = 0.5) but to maintain its velocity sufficiently low not to affect flame characteristics (<0.1 m/s).

The mass flow rate of a fuel and a coaxial air was controlled by a mass flow controller. The flow conditions studied here was chosen by combining fuel jet velocity, U_F, of 175, 245, 314 m/s and coaxial air velocity, U_A, of 5, 10, 20 m/s. Honeycombs provide a homogeneous flow. A speaker driver (Sammi, 150EF), attached to the bottom of the coaxial-jet tube and driven by an amplifier with a maximum output of 150 W, was used to excite the

coaxial air jet acoustically.

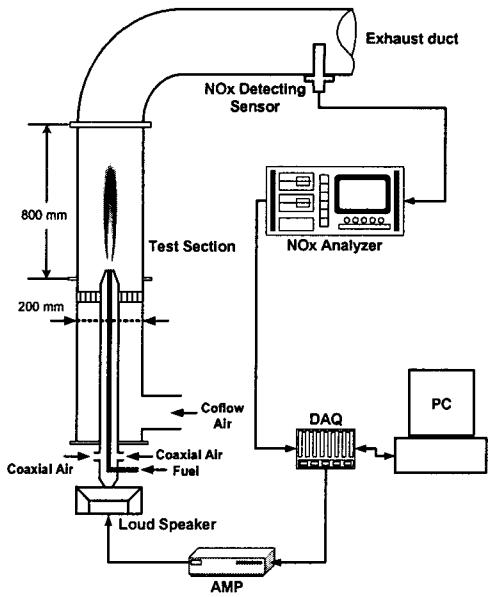

Fig. 1 The schematic of experimental setup

NOx measurements were performed using non-sampling type NOx analyzer with Zirconia-ceramic sensor (HORIBA, MEXA-720NOx). The sensor was directly inserted into the exhaust flow at 2-m downstream from the fuel nozzle, where the combustion product was found to be well-mixed with the dilution air. The emission index of NOx (EINOx) was used to correct the measured emission data of NOx, where EINOx for the hydrogen non-premixed flame was defined by the total grams of NOx produced when 1 kg of hydrogen is burned.

For particle image velocimetry (PIV) measurements, Seeding particles of nominally1-m TiO_2 were inserted into the fuel jet and the coaxial air jet. Two 532-nm Nd:YAG lasers were operating at a frequency of 9 Hz with 100 mJ per a pulse. The laser sheets formed by cylindrical lenses were illuminated into test section and then, the scattering signals from seeding particles were recorded on a high-resolution (1008×1018 pixels) Kodak ES1.0 CCD camera. The time separation between two laser pulses varies from 2 to 25 μs according to experimental conditions. The spatial resolution is 33.6 pixels per mm and the interrogation window size is 32 pixels by 32 pixels with 50 % overlap.

Acetone was seeded separately into the fuel jet and the coaxial air jet using a stainless steel atomizing nozzle. A frequency-quadrupled 266-nm Nd:YAG laser was used for acetone excitation. Fluorescence emitted from broad band was captured by an intensified CCD camera (Princeton Instrument, PI:MAX 1K), which resolution is 1024×1024 pixels with 16 bits. Acetone PLIF was carried out where the fluorescence signal shows a linear proportionality in order to prevent the saturation of the signal. Totally 200 images from each measurement of PIV and PLIF were phase-averaged synchronizing all the signals used here.

3. Results and Discussion

3.1 Resonance frequency effects

As randomly forcing frequencies from 0 to 1,000 Hz were imposed through the coaxial air nozzle, the acoustic pressure at the nozzle exit of the confined combustor was measured using a microphone. From the peak values in Fig. 2a, the longitudinal resonance frequencies were identified at 258, 514 and 750 Hz, which is nearly similar with 256.9, 523.8 and 770.6 Hz, the values calculated from theoretical estimation on the assumption that the schematic of the coaxial air tube is cylindrical [13].

Figure 2b shows the variation of NOx emissions according to the forcing frequencies with an acoustic power of 0.405 W in the flame of U_F=175 m/s and U_A=10 m/s. NOx concentration, X_{NOx}, of this case without acoustic excitation is 66 ppm. When a relatively weak acoustic power of 0.405 W is imposed at non-resonant frequencies, X_{NOx} is barely reduced by less than 1 ppm. However, at the resonance frequency of 514 Hz where higher acoustic amplitude is provided, X_{NOx} is decreased up to 62 ppm. This means that the resonance frequency determined by the burner geometry is more effective to amplify the forcing amplitude and reduce NOx emissions [11, 12]. Strongly forced acoustic excitation, however, may cause flame lift-off and blow-out [14], of which regions are of no interest because the present study is restricted

to the attached flames. Thus, the resonance frequency at 514 Hz was chosen to drive the coaxial air jet acoustically, with forcing amplitude not exceeding the limit of flame lift-off and blow-out regions.

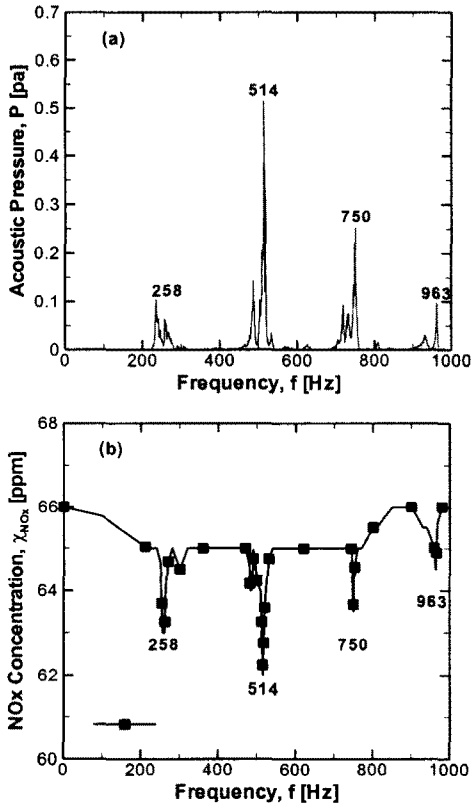

Fig. 2 (a) Acoustic pressure measured at the nozzle exit and (b) NOx concentration of U_F=175 m/s and U_A=10 m/s according to imposed acoustic frequency with P=0.405 W

3.2 Variation of flame length and NOx emission

Figure 3 shows a snapshot of Schlieren images captured by high-speed camera (3,000 fps) in the flame of U_F=175 m/s and U_A=5 m/s with and without acoustic excitation at forcing frequencies of 400 and 514 Hz. From the comparison of Fig. 3a and 3b, it is found that both Schlieren images are similar to each other, even if acoustic pulsing at non-resonant frequency of 400 Hz with 1.125 W is excited to the coaxial air jet in Fig. 3b. When acoustic forcing at resonance frequency of 514 Hz is excited with acoustic power of 1.125 W, Schlieren image of Fig. 3c is definitely distinguishable from the others because the characteristics of flow turn to be more turbulent. Thus, it is noted that it is more effective to excite the coaxial air jet at the specific frequency, which should be the resonance frequency determined from the burner geometry.

Fig. 3 The snapshot of Schlieren images in U_F=175 m/s and U_A=5 m/s without excitation and with acoustic excitation at the forcing frequency of 400 and 514 Hz with P=1.125 W.

Vortex pairing formed in the outer coaxial-jet side has a potential to affect global properties such as flame length and NOx emissions. Figure 4a describes the variations of normalized flame length, L_f/d_F, as a function of coaxial air to fuel velocity ratio, U_A/U_F, in coaxial air flames with and without acoustic excitation. Note that L_f is visual flame length and an acoustically forcing power is 1.125 W. In coaxial air flames without acoustic excitation, it was found that as coaxial air velocity increases, the flame length is reduced up to $80d_F$, which is about 45 % of $L_{f,0}$(=$180d_F$), ($L_{f,0}$ indicates the flame length of simple H_2 diffusion flames without coaxial air) [1, 2]. This is because coaxial air produces high mixing rate of fuel and air. When the forcing frequency of 514 Hz is excited to coaxial air jet with acoustic power of 1.125 W,

the flame length is getting even shorter than that without acoustic excitation and finally the additional 15 % reduction of the flame length is obtained.

To find the effect of acoustic excitation on the NOx emission, NOx measurements were also performed in coaxial air flames with and without acoustic excitation (same acoustic power as Fig. 4a). Figure 4b shows EINOx data have a similar tendency as the normalized flame length data. As coaxial air to fuel velocity ratio increases, EINOx decreases rapidly and an acoustic excitation reduces EINOx even more. For instance, EINOx is 17.0 for simple diffusion flames of U_F=175 m/s without coaxial air and it decreases to 8.2 if coaxial air of U_A=20 m/s is added into simple diffusion flame (U_A/U_F=0.114). If acoustic forcing is also added into coaxial air, EINOx is reduced to 6.2, which means that 64 % reduction in EINOx is achieved eventually. Further decrease in flame length and EINOx by acoustic excitation is closely related to mixing enhancement in the near field where streamwise vortex plays an important role.

3.3 Jet and flame behaviors interacted by vortices

A brief schematic of vortex structure is described in Fig. 5 to understand the mechanism of vortex interaction with mixing layer and flame surface studied in this work. When acoustic forcing is imposed, a streamwise vortex pair is periodically generated in the mixing layer between coaxial air jet and coflow air. The left half image of Fig. 5 is a raw image acquired from Mie scattering of seeding particles. In this study, strong streamwise vortex formed in the outer coaxial air jet boundary plays important roles, which are generally classified into three roles.

First, ambient coflowing air is entrained into the inner coaxial air jet. This entrained air is well-mixed with coaxial air during vortex roll-up, resulting in higher mixing rate. Second, flame surface is stretched by large vortex structure. In left half image of Fig. 5, a relatively dark region between fuel and coaxial air jet represents the region where reaction occurs and then, this dark region appears to be entrained outside as a vortex rolls up downstream. That is, the flame front is stretched by the outer vortex. Therefore, it is found that this flame stretching increases the flame area, resulting in intense chemical reactions. Finally, products formed in the upstream reaction zone are entrained into coaxial air jet as vortex rolls up downstream. As a result, combustion products could be mixed with a fresh air.

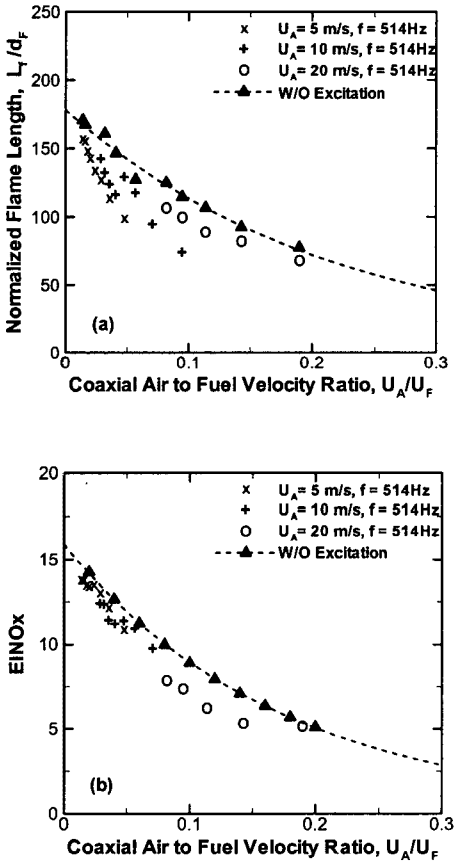

Fig. 4 (a) Normalized flame length and (b) EINOx variation in coaxial air flames with and without acoustic excitation at the forcing frequency of 514 Hz with P=1.125 W. Symbols 'x', '+', and 'o' means UA=5, 10, and 20 m/s respectively, with increasing UF with excitation. The dashed line indicates the cases without excitation.

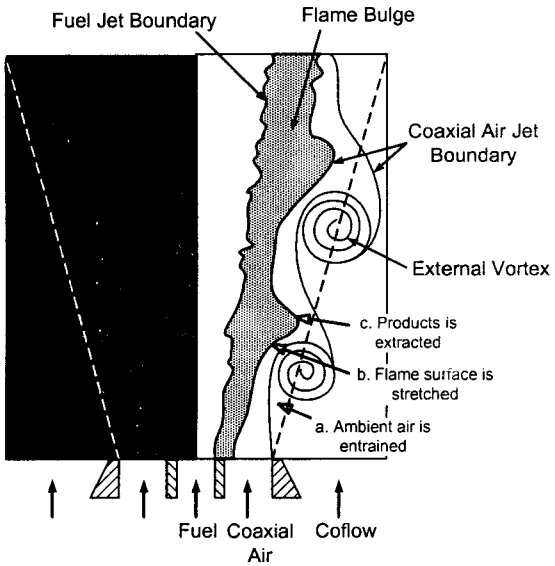

Fig. 5 TiO_2 Mie scattering image (left half) and schematic of flame-vortex interaction in an acoustically driven coaxial air flames at the resonance frequency of 514 Hz (right half).

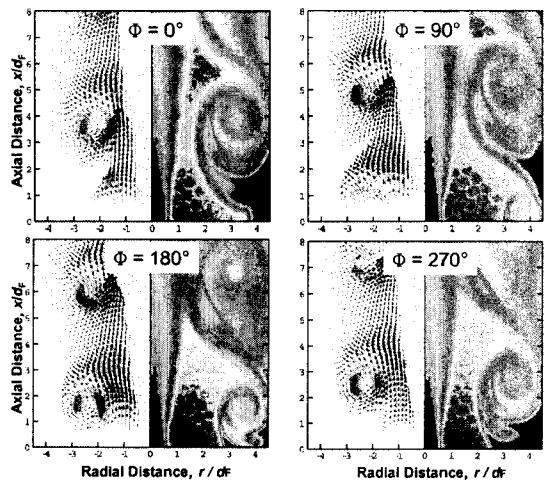

Fig. 6 Phase-locked velocity and acetone concentration fields in the nonreacting case of U_F=175 m/s and U_A=10 m/s at the forcing frequency of 514 Hz with P=1.125 W.

As shown in Fig. 6, velocity and concentration field measurements from PIV and acetone PLIF were conducted in the near field region of x/d_F=0.6 to 8 for the nonreacting case of U_F=175 m/s and U_A=10 m/s. Phase-lock average of 100 raw images was done fixed to the phase of the speaker input signal generated from a function generator. We can see that as the phase of the speaker signal increase the vortex grows and roll up gradually, showing that the size and strength of the vortex become larger and higher as the vortex goes downstream.

Figure 7 shows the pulsating radial velocity profiles of coaxial air according to the signal phases of Φ=0, 90, 180 and 270° at the measurement location of x/d_F=1. Reacting and nonreacting cases of U_F=175 m/s and U_A=10 m/s were carried out to figure out the differences and similarities for both cases. Forcing frequency and power are 514 Hz and 1.125 W, respectively. However, the fuel jet velocity is not displayed in Fig. 7 because the fuel velocity is much higher than the coaxial air velocity. The maximum velocity of about 12 m/s occurs at Φ=90° during each pulsation, while the minimum of about 8 m/s is at Φ= 270°, for both reacting and nonreacting cases. Coaxial air velocity fluctuates continuously by about ±2 m/s with respect to the average velocity of 10 m/s in response to the phases of acoustic pulsing.

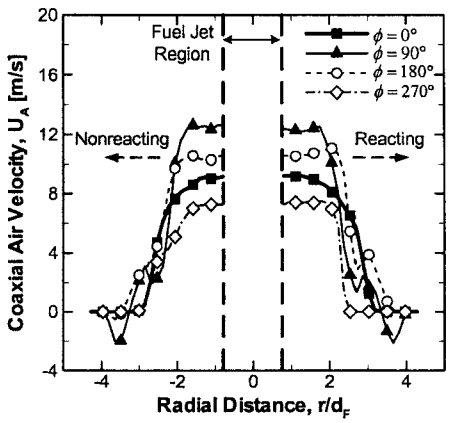

Fig. 7 The radial velocity profiles of coaxial air according the speaker phase in nonreacting (left half) and reacting (right half) cases of U_F=175 m/s and U_A=10 m/s at the forcing frequency of 514 Hz with P=1.125 W. The fuel jet region between the dashed lines is not displayed.

Large velocity fluctuation of coaxial air also can affect the fuel jet velocity, but in a little different way for reacting and nonreacting cases. As shown in Fig. 8a and 8b, the

centerline fuel velocity, $U_{F,C}$, tend to decay proportional to x^{-1} and the fuel velocity fluctuates as the phase varies. For example, the velocity fluctuations between maximum to minimum of $U_{F,C}$ are about 26 m/s at x/d_F=3 for nonreacting case and about 37 m/s at x/d_F=5 for reacting case. However, the peak of fuel velocity fluctuations is observed at the different phases unlike that of coaxial case: ϕ =180° for nonreacting case, ϕ=0° for reacting case.

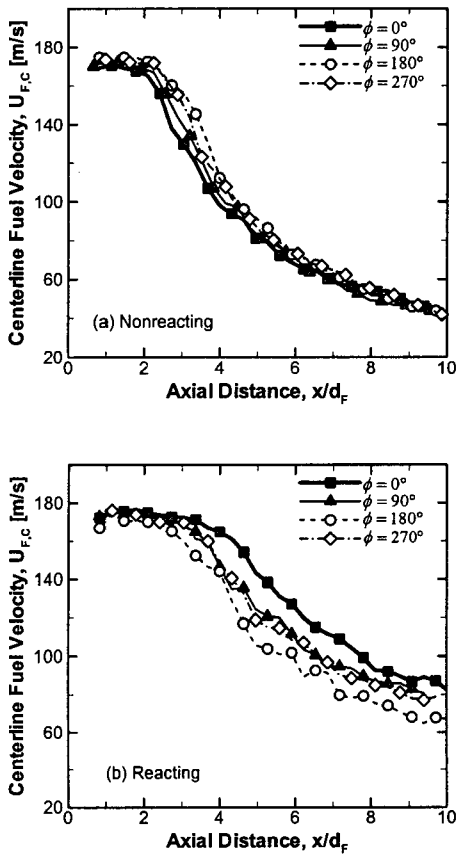

Fig. 8 The decay of centerline fuel velocity, $U_{F,C}$, along the axial distance at different speaker phases in (a) nonreacting and (b) reacting cases of U_F=175 m/s and U_A=10 m/s at the forcing frequency of 514 Hz with P=1.125 W.

This phase difference between velocity fluctuations of reacting and nonreacting cases can be explained from Fig. 11, which indicates the growth rate of jet width, D_{FWHM}, defined as full-width at half maximum (FWHM) for nonreacting and reacting cases. In nonreacting case, momentum rate of coaxial air is increased with increasing the phase due to velocity fluctuation and reaches its peak at =90°. At that moment, coaxial air jet pushes fuel jet inside and after that, jet width becomes narrower. Therefore, centerline fuel velocity begins to increase and becomes maximum at ϕ=180° where jet width is relatively a little narrower than that at ϕ=0° as shown in Fig. 9.

In reacting case, however, there exists flame surface in the mixing layer between fuel and coaxial air jet. Contrary to nonreacting case, coaxial air jet fluctuated by acoustic forcing does not go through fuel jet owing to thermal expansion. But, a vortex pair is formed in the mixing layer between coaxial air and coflow. As vortex rolls up downstream, it pulls the flame surface into the outer coaxial air jet. Therefore, jet width becomes broader and at ϕ =180° where jet width is relatively broader than that at ϕ=0°.

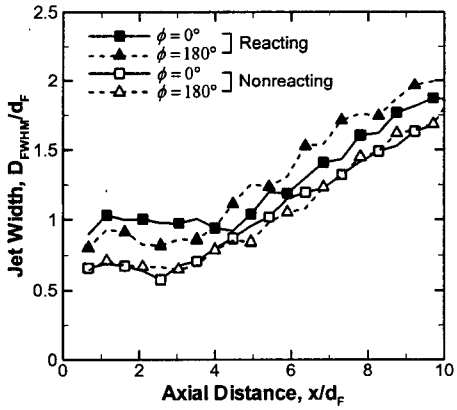

Fig. 9 The growth rate of jet width, D_{FWHM}, along the axial distance in nonreacting and reacting cases of U_F=175 m/s and U_A=10 m/s.

Now, the characteristics of vortical structure were examined from the velocity field obtained by the PIV technique. The rotating velocity, U_θ, of a vortex caused by acoustic forcing was considered as maximum of axial velocity across a vortex. For the nonreacting case of Fig. 10a, U_θ, increases up to about 7 m/s, then decreases gradually with increasing the axial distance. Note that the phase difference

between two data points of rotating velocity is 90°. Although the phase of a vortex increases each 90°, the axial distance of each data points is almost equal. This fact indicates that a vortex occurred by acoustic forcing goes downstream with a constant convective velocity. For the reacting case of Fig. 10b, merging phenomenon of two consecutive vortices happens. That is, first vortex is formed and then goes downstream. After a certain time interval, second vortex is also formed but goes downstream faster than fist vortex does. Thus, at further downstream, first vortex is caught by second one and these two vortices are merged into large one.

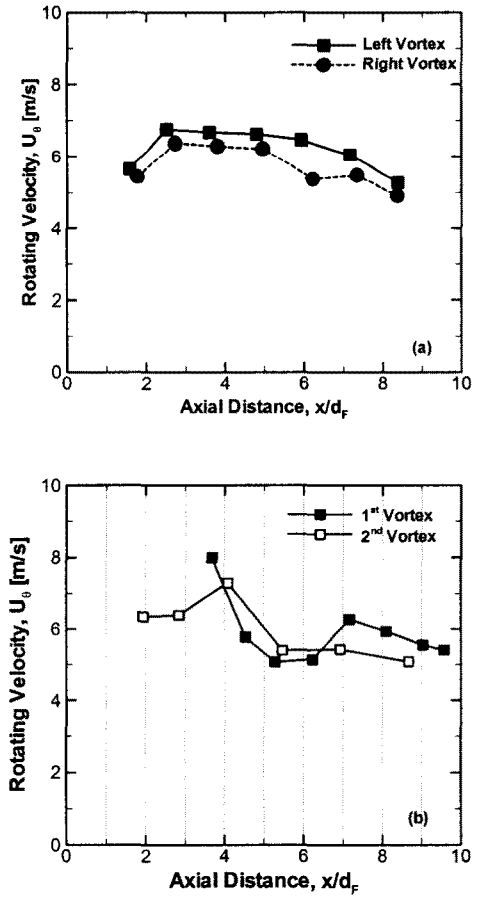

Fig. 10 The variations of rotating velocity along the axial distance. (a) Nonreacting and (b) reacting cases of U_F=175 m/s and U_A=10 m/s.

The probability density function of maximum vorticity of a vortex can also be extracted from post- processing of the velocity field. As shown in Fig. 11, the vorticity of a vortex ranges from 10,000 to 30,000 s^{-1} for both nonreacting and reacting cases. The peak value of maximum vorticity is about 16,000 s^{-1} regardless of axial location of the vortex.

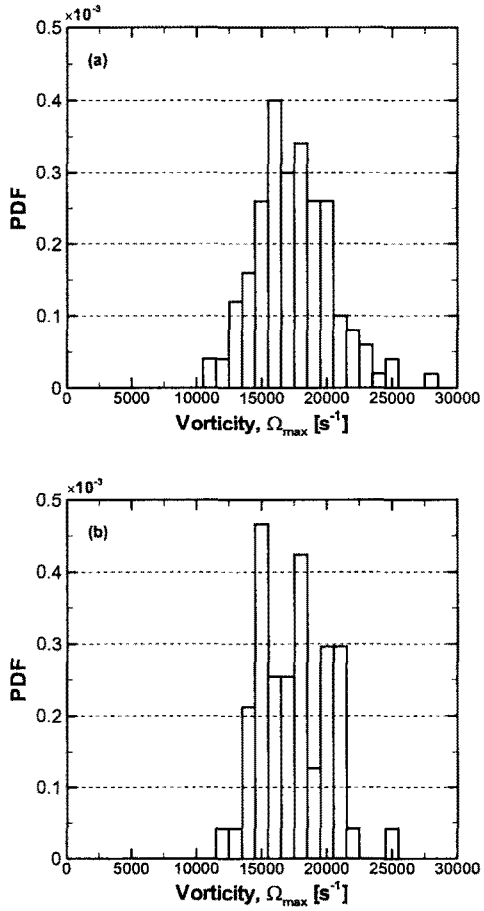

Fig. 11 The PDF of maximum vorticity of a vortex at Φ=180°. (a) Nonreacting and (b) reacting cases of U_F=175 m/s and U_A=10 m/s.

4. Conclusions

To investigate the dynamic behaviors in the near field of turbulent hydrogen nonpremixed flames by acoustically resonant coaxial air, experimental measurements of NOx, velocity field, concentration field were conducted. The resonance frequency was selected to force the

coaxial air jet acoustically, because the resonance frequency is effective to amplify the forcing amplitude and reduce NOx emissions. When acoustic pulsing at the resonance frequency is imposed, a streamwise vortex is formed in the mixing layer between coaxial air jet and coflow air. Acoustic excitation causes velocity fluctuations of coaxial air jet as well as fuel jet but the maximum value of centerline fuel velocity fluctuation occurs at the different phases of ϕ=180° for nonreacting case and ϕ=0° for reacting case. Since acoustic excitation enhances the mixing rate of fuel and air, the line of the stoichiometric mixture fraction becomes narrow. Finally, as acoustic forcing is imposed with the same acoustic power, the normalized flame length is reduced by 15 % and consequently, additional 25 % reduction in EINOx is achieved, compared to the flame without acoustic excitation.

From TiO_2 Mie scattering image, it can be inferred that as a streamwise vortex generated in the mixing layer between coaxial air jet and coflow air rolls up downstream, it entrains ambient coflow air into the coaxial air jet and extracts combustion products out of the flame region as well. Furthermore, the strong vortex pulls the flame surface toward the coaxial air jet, resulting in increasing flame area. Consequently, these mixing processes may be closely related to NOx reduction by acoustically resonant coaxial air.

Reference

[1] Chen, R.-H. and Driscoll, J. F., "Nitric oxide levels of jet diffustion flames: effects of coaxial air and other mixing parameters," Proc. Combust. Inst., 23, (1990), 281-288.

[2] Kim, S. H., Yoon, Y. and Jeung, I.S., "Nitrogen oxides emissions in turbulent hydrogen jet non-premixed flames: effects of coaxial air and flame radiation," Proc. Combust. Inst., 28 (2000), 463-471.

[3] Kim, S. H., Kim, M., Yoon, Y. and Jeung, I. S., The effect of flame radiation on the scaling of nitrogen oxide emissions in turbulent hydrogen non-premixed flames, Proc. Combust. Inst., 29 (2002), 1951-1956.

[4] Renard, P. -H., Th?venin, D., Rolon, J. C. and Candel, S., Dynamics of flame/vortex interactions, Prog. Ener. Combust. Sci., 26 (2000), 225-282.

[5] Meyer, T. R., Dutton, J. C. and Lucht, R. P., Vortex interaction and mixing in a driven gaseous axisymmetric jet, Phys. Fluid, 11-11 (1999), 3401-3415.

[6] Katta, V. R. and Roquemore, W. M., On the structure of a stretched/compressed laminar flamelet - influence of preferential diffusion, Combust. Flame, 100 (1995), 61-70.

[7] Mueller, C. J. and Schefer, R. W., Coupling of diffusion flame structure to an unsteady vortical flow-field, Proc. Combust. Inst., 27 (1998), 1105-1112.

[8] Takahashi, F., Schmoll, W. J., Trump, D. D. and Goss, L. P., Vortex-flame interactions and extinction in turbulent jet diffusion flames, Proc. Combust. Inst., 26 (1996), 145-152.

[9] Zheng, X. L., Yuan, J. and Law, C. K., Nonpremixed ignition of H2/air in a mixing layer with a vortex, Proc. Combust. Inst., 30 (2004), 415-421.

[10] Chao, Y. -C., Yuan, T. and Tseng, C. -S., Effects of flame lifting and acoustic excitation on the reduction of NOx emissions, Combust. Sci. Technol., 113-114 (1996), 49-65.

[11] Parr, T. P., Gutmark, E., Wilson, K., Hanson-Parr, D. M., Yu, K., Smith, R. A. and Schadow, K. C., Compact incinerator afterburner concept based on vortex combustion, Proc. Combust. Inst., 26 (1996), 2471-2477.

[12] Pont, G., Willis, J. W., Karagozian, A. R. and Smith, O. I., Effects of external acoustic excitation on enhanced transport in a resonant incinerator, Proc. Combust. Inst., 26 (1996), 2463-2470.

[13] Zucrow, M.J., Hoffman, J.D., Gas Dynamics Vol. II: Multimedia Flow. John Wiley & Sons, 1997.

[14] Demare, D. and Baillot, F., Acoustic enhancement of combustion in lifted nonpremixed jet flames, Combust. Flame, 139 (2004), 312-328.